

Perturbation Bounds for Procrustes, Classical Scaling, and Trilateration, with Applications to Manifold Learning

Ery Arias-Castro*

Adel Javanmard†

Bruno Pelletier‡

November 16, 2021

Abstract

One of the common tasks in unsupervised learning is dimensionality reduction, where the goal is to find meaningful low-dimensional structures hidden in high-dimensional data. Sometimes referred to as manifold learning, this problem is closely related to the problem of localization, which aims at embedding a weighted graph into a low-dimensional Euclidean space. Several methods have been proposed for localization, and also manifold learning. Nonetheless, the robustness property of most of them is little understood. In this paper, we obtain perturbation bounds for classical scaling and trilateration, which are then applied to derive performance bounds for Isomap, Landmark Isomap, and Maximum Variance Unfolding. A new perturbation bound for procrustes analysis plays a key role.

1 Introduction

Multidimensional scaling (MDS) can be defined as the task of embedding an itemset as points in a (typically) Euclidean space based on some dissimilarity information between the items in the set. Since its inception, dating back to the early 1950’s if not earlier [41], MDS has been one of the main tasks in the general area of multivariate analysis, a.k.a., unsupervised learning.

One of the main methods for MDS is called classical scaling, which consists in first double-centering the dissimilarity matrix and then performing an eigen-decomposition of the obtained matrix. This is arguably still the most popular variant, even today, decades after its introduction at the dawn of this literature. (For this reason, this method is often referred to as MDS, and we will do the same on occasion.) Despite its wide use, its perturbative properties remain little understood. The major contribution on this question dates back to the late 1970’s with the work of Sibson [26], who performs a sensitivity analysis that resulted in a Taylor development for the classical scaling to the first nontrivial order. Going beyond Sibson [26]’s work, our first contribution is to derive a bonafide perturbation bound for classical scaling (Theorem 2).

Classical scaling amounts to performing an eigen-decomposition of the dissimilarity matrix after double-centering. Only the top d eigenvectors are needed if an embedding in dimension d is desired. Using iterative methods such as the Lanczos algorithm, classical scaling can be implemented with a complexity of $O(dn^2)$, where n is the number of items (and therefore also the dimension of the dissimilarity matrix). In applications, particularly if the intent is visualization, the embedding dimension d tends to be small. Even then, the resulting complexity is quadratic in the number of

*Department of Mathematics, University of California, San Diego

†Marshall School of Business, University of Southern California

‡Département de Mathématiques, IRMAR - UMR CNRS 6625, Université Rennes II

items n to be embedded. There has been some effort in bringing this down to a complexity that is linear in the number of items. The main proposals [8, 10, 35] are discussed by Platt [23], who explains that all these methods use a Nyström approximation. The procedure proposed by de Silva and Tenenbaum [8], which they called landmark MDS (LMDS) and which according to Platt [23] is the best performing methods among these three, works by selecting a small number of items, perhaps uniformly at random from the itemset, and embedding them via classical scaling. These items are used as landmark points to enable the embedding of the remaining items. The second phase consists in performing trilateration, which aims at computing the location of a point based on its distances to known (landmark) points. Note that this task is closely related to, but distinct, from triangulation, which is based on angles instead. If ℓ items are chosen as landmarks in the first step (out of n items in total), then the procedure has complexity $O(d\ell^2 + d\ell n)$. Since ℓ can in principle be chosen on the order of d , and $d \leq n$ always, the complexity is effectively $O(d^2 n)$, which is linear in the number of items. A good understanding of the robustness properties of LMDS necessitates a good understanding of the robustness properties of not only classical scaling (used to embed the landmark items), but also of trilateration (used to embed the remaining items). Our second contribution is a perturbation bound for trilateration (Theorem 3). There are several closely related method for trilateration, and we study on the method proposed by de Silva and Tenenbaum [8], which is rather natural. We refer to this method simply as trilateration in the remaining of the paper.

de Silva and Tenenbaum [8] build on the pioneering work of Sibson [26] to derive a sensitivity analysis of classical scaling. They also derive a sensitivity analysis for their trilateration method following similar lines. In the present work, we instead obtain bona fide perturbation bounds, for procrustes analysis (Section 2), for classical scaling (Section 3), and for the same trilateration method (Section 4). In particular, our perturbation bounds for procrustes analysis and classical scaling appear to be new, which may be surprising as these methods have been in wide use for decades. (The main reason for deriving a perturbation bound for procrustes analysis is its use in deriving a perturbation bound for classical scaling, which was our main interest.) These results are applied in Section 5 to Isomap, Landmark Isomap, and also Maximum Variance Unfolding (MVU). These may be the first performance bounds of any algorithm for manifold learning in its ‘isometric embedding’ variant, even as various consistency results have been established for Isomap [42], MVU [2], and a number of other methods [3, 6, 9, 13, 15, 27, 28, 34, 40]. (As discussed in [14], Local Linear Embedding, Laplacian Eigenmaps, Hessian Eigenmaps, and Local Tangent Space Alignment, all require some form of normalization which make them inconsistent for the problem of isometric embedding.) In Section 6 we discuss the question of optimality in manifold learning and also the choice of landmarks. The main proofs are gathered in Section 7.

2 A perturbation bound for procrustes

The orthogonal procrustes problem is that of aligning two point sets (of same cardinality) using an orthogonal transformation. In formula, given two point sets, x_1, \dots, x_m and y_1, \dots, y_m in \mathbb{R}^d , the task consists in solving

$$\min_{Q \in \mathcal{O}(d)} \sum_{i=1}^m \|y_i - Qx_i\|^2, \quad (1)$$

where $\mathcal{O}(d)$ denotes the orthogonal group of \mathbb{R}^d . (Here and elsewhere, when applied to a vector, $\|\cdot\|$ will denote the Euclidean norm.)

In matrix form, the problem can be posed as follows. Given matrices X and Y in $\mathbb{R}^{m \times d}$, solve

$$\min_{Q \in \mathcal{O}(d)} \|Y - XQ\|_2, \quad (2)$$

where $\|\cdot\|_2$ denotes the Frobenius norm (in the appropriate space of matrices). As stated, the problem is solved by choosing $Q = UV^\top$, where U and V are d -by- d orthogonal matrices obtained by a singular value decomposition of $X^\top Y = UDV^\top$, where D is the diagonal matrix with the singular values on its diagonal [24, Sec 5.6]. Algorithm 1 describes the procedure.

Algorithm 1 Procrustes (Frobenius norm)

Input: point sets x_1, \dots, x_m and y_1, \dots, y_m in \mathbb{R}^d

Output: an orthogonal transformation Q of \mathbb{R}^d

1: store the point sets in $X = [x_1^\top \cdots x_m^\top]$ and $Y = [y_1^\top \cdots y_m^\top]$

2: compute $X^\top Y$ and its singular value decomposition UDV^\top

Return: the matrix $Q = UV^\top$

In matrix form, the problem can be easily stated using any other matrix norm in place of the Frobenius norm. There is no closed-form solution in general, even for the operator norm (as far as we know), although some computational strategies have been proposed for solving the problem numerically [36]. In what follows, we consider an arbitrary Schatten norm. For a matrix $A \in \mathbb{R}^{m \times n}$, let $\|A\|_p$ denote the Schatten p -norm, where $p \in [1, \infty]$ is assumed fixed:

$$\|A\|_p \equiv \left(\sum_{i \geq 1} \nu_i^p(A) \right)^{1/p}, \quad (3)$$

with $\nu_1(A) \geq \nu_2(A) \geq \dots \geq 0$ the singular values of A . Note that $\|\cdot\|_2$ coincides with the Frobenius norm. We also define $\|A\|_\infty$ to be the usual operator norm, i.e., the maximum singular value of A . Henceforth, we will also denote the operator norm by $\|\cdot\|$, on occasion. We denote by A^\ddagger the pseudo-inverse of A (see Section 7.1).

Theorem 1. Consider two tall matrices X and Y of same size, with X having full rank, and set $\varepsilon^2 = \|YY^\top - XX^\top\|_p$. If $\|X^\ddagger\|\varepsilon \leq \frac{1}{\sqrt{2}}(\|X\|\|X^\ddagger\|)^{-1/2}$, then

$$\min_{Q \in \mathcal{O}} \|Y - XQ\|_p \leq (\|X\|\|X^\ddagger\| + 2)\|X^\ddagger\|\varepsilon^2. \quad (4)$$

The proof is in Section 7.2. Interestingly, to establish the upper bound we use an orthogonal matrix constructed from the singular value decomposition of $X^\ddagger Y$. This is true regardless of p , which may be surprising since a solution for the Frobenius norm (corresponding to the case where $p = 2$) is based on a singular value decomposition of $X^\top Y$ instead.

Remark 1. The case where X and Y are orthogonal is particularly simple, at least when $p = 2$ or $p = \infty$, based on what is already known in the literature. Indeed, from [30, Sec II.4] we find that, in that case,

$$\min_{Q \in \mathcal{O}} \|Y - XQ\|_p = \|2 \sin(\frac{1}{2}\theta(X, Y))\|_p, \quad (5)$$

where $\theta(X, Y)$ is the diagonal matrix made of the principal angles between the subspaces defined by X and Y , while

$$\varepsilon^2 = \|YY^\top - XX^\top\|_p = \|\sin \theta(X, Y)\|_p. \quad (6)$$

Using the elementary inequality $\sqrt{2}\sin(\alpha/2) \leq \sin(\alpha) \leq 2\sin(\alpha/2)$, valid for $\alpha \in [0, \pi/2]$, we get

$$\varepsilon^2 \leq \min_{Q \in \mathcal{O}} \|Y - XQ\|_p \leq \sqrt{2}\varepsilon^2. \quad (7)$$

Note that, in this case, $\|X\| = \|X^\dagger\| = 1$, and compare with our (upper) bound.

Remark 2. Our result applies when $\|X^\dagger\|\varepsilon$ is sufficiently small relative to the inverse of the condition number of X . In our proof, we obtain a sharper bound in (57) which does not strictly require that, but even then the bound becomes essentially useless if $\|X^\dagger\|\varepsilon$ is large. As it turns out, the result as stated in Theorem 1 will be enough for our purposes, but we do conjecture that there is a smooth transition between a bound in ε^2 and a bound in ε as $\|X^\dagger\|$ increases to infinity (and therefore X degenerates to a singular matrix).

3 A perturbation bound for classical scaling

In multidimensional scaling, we are given a matrix, $\Delta = (\Delta_{ij}) \in \mathbb{R}^{m \times m}$, storing the dissimilarities between a set of m items (which will remain abstract in this paper). In particular, Δ_{ij} gives the level of dissimilarity between items $i, j \in [m]$. We will assume throughout that the dissimilarities are non-negative. Given a positive integer d , we seek a configuration, meaning a set of points, $y_1, \dots, y_m \in \mathbb{R}^d$, such that $\|y_i - y_j\|^2$ is close to Δ_{ij} over all $i, j \in [m]$. The itemset $[m]$ is thus embedded as y_1, \dots, y_m in the d -dimensional Euclidean space \mathbb{R}^d . Algorithm 2 describes classical scaling, the most prominent method for solving this problem. In the description, $H = I - J/m$ is the centering matrix in dimension m , where I is the identity matrix and J is the matrix of ones. The method is widely attributed to Torgerson [32].

Algorithm 2 Classical Scaling

Input: dissimilarity matrix $\Delta \in \mathbb{R}^{m \times m}$, embedding dimension d

Output: set of points $y_1, \dots, y_m \in \mathbb{R}^d$

1: compute the matrix $\Delta^c = -\frac{1}{2}H\Delta H$

2: compute $Y \in \mathbb{R}^{m \times d}$ such that $YY^\top = \Delta^c$

Return: the row vectors y_1, \dots, y_m of Y

The rationale behind the classical scaling is the following identity regarding a configuration X and the corresponding squared distance matrix Δ :

$$-\frac{1}{2}H\Delta H = HXX^T H. \quad (8)$$

Consider the situation where the dissimilarity matrix Δ is exactly realizable in dimension d , meaning that there is a set of points y_1, \dots, y_m such that $\Delta_{ij} = \|y_i - y_j\|^2$. It is worth noting that, in that case, the set of points that perfectly embed Δ in dimension d are rigid transformations of each other. It is well-known that classical scaling provides such a set of points which happens to be centered at the origin (see Eq. 8).

We perform a perturbation analysis of classical scaling, by studying the effect of perturbing the dissimilarities on the embedding that the algorithm returns. This sort of analysis helps quantify the degree of robustness of a method to noise, and is particularly important in applications where the dissimilarities are observed with some degree of inaccuracy, which is the case in the context of manifold learning (Section 5.1). Recall that \mathcal{O} denotes the orthogonal group of matrices of a proper size that will be clear from the context.

Theorem 2. Consider a centered and full-rank configuration $Y \in \mathbb{R}^{m \times d}$ with dissimilarity matrix Δ . Let Λ denote another dissimilarity matrix and set $\varepsilon^2 = \frac{1}{2}\|H(\Lambda - \Delta)H\|_p$. If it holds that $\|Y^\ddagger\|\varepsilon \leq \frac{1}{\sqrt{2}}(\|Y\|\|Y^\ddagger\|)^{-1/2}$, then classical scaling with input dissimilarity matrix Λ and dimension d returns a centered configuration $Z \in \mathbb{R}^{m \times d}$ satisfying

$$\min_{Q \in \mathcal{O}} \|Z - YQ\|_p \leq (\|Y\|\|Y^\ddagger\| + 2)\|Y^\ddagger\|\varepsilon^2. \quad (9)$$

We note that $\varepsilon^2 \leq \frac{1}{2}d^{2/p}\|\Lambda - \Delta\|_p$, after using the fact that $\|H\|_p = (d-1)^{1/p}$ since H has one zero eigenvalue and $d-1$ eigenvalues equal to one.

Proof. We have

$$\|\Lambda^c - \Delta^c\|_p = \frac{1}{2}\|H(\Lambda - \Delta)H\|_p = \varepsilon^2. \quad (10)$$

Noting that $\Delta^c = YY^\top$ and $\Lambda^c = ZZ^\top$, we simply apply Theorem 1, which we can do since Y has full rank by assumption, to conclude. \square

Remark 3. This perturbation bound is optimal in how it depends on ε . Indeed, suppose without loss of generality that $p = 2$. (All the Schatten norms are equivalent modulo constants that depend on d and p .) Consider a configuration Y as in the statement, and define $Z = (1+a)Y$ where $0 \leq a \leq 1$. On the one hand, we have [24, Sec 5.6]

$$\min_{Q \in \mathcal{O}} \|Z - YQ\|_2 = \|Z - Y\|_2 = a\|Y\|_2. \quad (11)$$

On the other hand,

$$\varepsilon^2 = \|ZZ^\top - YY^\top\|_2 = ((1+a)^2 - 1)\|YY^\top\|_2, \quad (12)$$

so that the right-hand side in (9) is bounded by $9a\|Y\|\|Y^\ddagger\|^2\|YY^\top\|_2$, using $\|Y\|\|Y^\ddagger\| \geq 1$ and $a \in [0, 1]$. We therefore conclude that the ratio of the left-hand side to the right-hand side in (9) is at least

$$\frac{a\|Y\|_2}{9a\|Y\|\|Y^\ddagger\|^2\|YY^\top\|_2} \geq \frac{1}{9}(\|Y\|\|Y^\ddagger\|)^{-2}, \quad (13)$$

using the fact that $\|YY^\top\|_2 \leq \|Y\|\|Y\|_2$. Therefore, our bound (9) is tight up to a multiplicative factor depending on the condition number of the configuration Y .

We now translate this result in terms of point sets instead of matrices. For a centered point set $y_1, \dots, y_m \in \mathbb{R}^d$, stored in the matrix $Y = [y_1 \dots y_m]^\top \in \mathbb{R}^{m \times d}$, define its radius as the largest standard deviation along any direction in space (therefore corresponding to the square root of the top eigenvalue of the covariance matrix). We denote this by $\rho(Y)$ and note that

$$\rho(Y) = \|Y\|/\sqrt{m}. \quad (14)$$

We define its half-width as the smallest standard deviation along any direction in space (therefore corresponding to the square root of the bottom eigenvalue of the covariance matrix). We denote this by $\omega(Y)$ and note that it is strictly positive if and only if the point set spans the whole space, in which case

$$\omega(Y) = \|Y^\ddagger\|^{-1}/\sqrt{m}. \quad (15)$$

It is well-known that the half-width quantifies the best affine approximation to the point set, in the sense that

$$\omega(Y)^2 = \min_{\mathcal{L}} \frac{1}{m} \sum_{i \in [m]} \|y_i - P_{\mathcal{L}}y_i\|^2, \quad (16)$$

where the minimum is over all affine hyperplanes \mathcal{L} , and for a subspace \mathcal{L} , $P_{\mathcal{L}}$ denotes the orthogonal projection onto \mathcal{L} . We note that $\rho(Y)/\omega(Y) = \|Y\|\|Y^\dagger\|$ is the aspect ratio of the point set.

Corollary 1. *Consider a centered point set $y_1, \dots, y_m \in \mathbb{R}^d$ with radius ρ , and with half-width ω , and with pairwise dissimilarities $\delta_{ij} = \|y_i - y_j\|^2$. Consider another set of dissimilarities $\{\lambda_{ij}\}$ and set $\eta^4 = \frac{1}{m^2} \sum_{i,j} (\lambda_{ij} - \delta_{ij})^2$. If $\eta/\omega \leq (\rho/\omega)^{-1/2}$, then classical scaling with input dissimilarities $\{\lambda_{ij}\}$ and dimension d returns a point set $z_1 \dots z_m \in \mathbb{R}^d$ satisfying*

$$\min_{Q \in \mathcal{O}} \left(\frac{1}{m} \sum_{i \in [m]} \|z_i - Qy_i\|^2 \right)^{1/2} \leq \frac{\sqrt{d}(\rho/\omega + 2)}{2\omega} \eta^2 \leq \frac{2\sqrt{d}\rho\eta^2}{\omega^2}. \quad (17)$$

This corollary follows from Theorem 2. We refer to Section 7.4 for its proof.

4 A perturbation bound for trilateration

The problem of trilateration is that of positioning a point, or set of points, based on its (or their) distances to a set of points, which in this context serve as landmarks. In detail, given a set of landmark points $y_1, \dots, y_m \in \mathbb{R}^d$ and a set of dissimilarities $\delta_1, \dots, \delta_m$, the goal is to find $x \in \mathbb{R}^d$ such that $\|x - y_i\|^2$ is close to δ_i over all $i \in [m]$. Algorithm 3 describes the trilateration method of de Silva and Tenenbaum [8] simultaneously applied to multiple points to be located. The procedure is shown in [8] to be exact when the point set spans the whole space, but we provide a more succinct proof of this in the Section A.1.

Algorithm 3 Trilateration

Input: centered point set $y_1, \dots, y_m \in \mathbb{R}^d$, dissimilarities $\Delta = (\delta_{ij}) \in \mathbb{R}^{n \times m}$

Output: points $x_1, \dots, x_n \in \mathbb{R}^d$

1: compute $\bar{a} = \frac{1}{m} \sum_{i=1}^m a_i$, where $a_i = (\|y_i - y_1\|^2, \dots, \|y_i - y_m\|^2)$

2: compute the pseudo-inverse Y^\dagger of $Y = [y_1 \dots y_m]^\top$

3: compute $X^\top = \frac{1}{2} Y^\dagger (\bar{a} 1^\top - \Delta^\top)$

Return: the row vectors of X , denoted $x_1, \dots, x_n \in \mathbb{R}^d$

We perturb both the dissimilarities and the landmark points, and qualitatively characterize how it will affect the returned positions by trilateration. (In principle, the perturbed point set need not have the same mean as the original point set, but we assume this is the case, for simplicity and because it suffices for our application of this result in Section 5.) For a configuration $Y = [y_1 \dots y_m]^\top$, define its max-radius as

$$\rho_\infty(Y) = \max_{i \in [m]} \|y_i\|, \quad (18)$$

and note that $\rho(Y) \leq \rho_\infty(Y)$. We content ourselves with a bound in Frobenius norm.¹

Theorem 3. *Consider a centered configuration $Y \in \mathbb{R}^{m \times d}$ that spans the whole space, and for a given configuration $X \in \mathbb{R}^{n \times d}$, let $\Delta \in \mathbb{R}^{n \times m}$ denote the matrix of dissimilarities between X and Y . Let $Z \in \mathbb{R}^{m \times d}$ be another centered configuration that spans the whole space, and let $\Theta \in \mathbb{R}^{n \times m}$ be*

¹ All Schatten norms are equivalent here up to a multiplicative constant that depends on d , since the matrices that we consider have rank of order d .

an arbitrary matrix of dissimilarities. Then, trilateration with inputs Z and Θ returns $\tilde{X} \in \mathbb{R}^{n \times d}$ satisfying

$$\begin{aligned} \|\tilde{X} - X\|_2 &\leq \frac{1}{2} \|Z^\dagger\| \|\Theta - \Delta\|_2 + 2\|X\| \|Z^\dagger\| \|Z - Y\|_2 \\ &\quad + \frac{3}{2} \sqrt{m} (\rho_\infty(Y) + \rho_\infty(Z)) \|Z^\dagger\| \|Z - Y\|_2 + \|Y\| \|X\| \|Z^\dagger - Y^\dagger\|_2. \end{aligned} \quad (19)$$

Remark 4. The right-hand side of (19) can be upper bounded using

$$\rho_\infty(Z) \leq \rho_\infty(Y) + \rho_\infty(Z - Y), \quad \|Z^\dagger\| \leq \|Y^\dagger\| + \|Z^\dagger - Y^\dagger\|, \quad (20)$$

and

$$\|Z^\dagger - Y^\dagger\|_p \leq \frac{\sqrt{2} \|Y^\dagger\|^2 \|Z - Y\|_p}{(1 - \|Y^\dagger\| \|Z - Y\|)^2_+}, \quad p \in \{2, \infty\}, \quad (21)$$

as per Lemma 2. Also, a simple application of Mirksky's inequality (43) implies that, when Y spans the whole space then so does Z whenever $\|Y^\dagger\| \|Z - Y\| < 1$.

The proof is in Section 7.3. We now derive from this result another one in terms of point sets instead of matrices.

Corollary 2. Consider a centered point set $y_1, \dots, y_m \in \mathbb{R}^d$ with radius ρ , max-radius ρ_∞ , and half-width $\omega > 0$. For a point set $x_1, \dots, x_n \in \mathbb{R}^d$ with radius ζ , set $\delta_{ij} = \|x_i - y_j\|^2$. Also, let $z_1, \dots, z_m \in \mathbb{R}^d$ denote another centered point set, and let (θ_{ij}) denote another set of dissimilarities. Set $\varepsilon = \max_{i \in [m]} \|z_i - y_i\|$ and $\eta^4 = \frac{1}{nm} \sum_{ij} (\theta_{ij} - \delta_{ij})^2$. If $\varepsilon \leq \omega/2$, trilateration with inputs z_1, \dots, z_m and (θ_{ij}) returns $\tilde{x}_1, \dots, \tilde{x}_n \in \mathbb{R}^d$ satisfying

$$\left(\frac{1}{n} \sum_{i \in [n]} \|\tilde{x}_i - x_i\|^2 \right)^{1/2} \leq C_0 \left(\frac{\eta^2}{\omega} + \left[\frac{\rho \zeta}{\omega^2} + \frac{\sqrt{m} \rho_\infty}{\sqrt{n} \omega} \right] \varepsilon \right), \quad (22)$$

where C_0 is a universal constant.

Corollary 2 follows from Theorem 3 and its proof is given in Section 7.5.

5 Applications to manifold learning

Consider a set of points in a possibly high-dimensional Euclidean space, that lie on a smooth Riemannian manifold. Isometric manifold learning (or embedding) is the problem of embedding these points into a lower-dimensional Euclidean space, and do as while preserving as much as possible the Riemannian metric. There are several variants of the problem under other names, such as nonlinear dimensionality reduction.

Remark 5. Manifold learning is intimately related to the problem of embedding items with only partial dissimilarity information, which practically speaking means that some of the dissimilarities are missing. We refer to this problem as graph embedding below, although it is known under different names such as graph realization, graph drawing, and sensor localization. This connection is due to the fact that, in manifold learning, the short distances are nearly Euclidean, while the long distances are typically not. In fact, the two methods for manifold learning that we consider below can also be used for graph embedding. The first one, Isomap [31], coincides with MDS-MAP [25] (see also [21]), although the same method was suggested much earlier by Kruskal and Seery [20]; the second one, Maximum Variance Unfolding, was proposed as a method for graph embedding by the same authors [39], and is closely related to other graph embedding methods [5, 18, 29].

Algorithm 4 Isomap

Input: data points $x_1, \dots, x_n \in \mathbb{R}^D$, embedding dimension d , neighborhood radius r

Output: embedding points $y_1, \dots, y_n \in \mathbb{R}^d$

1: construct the graph on $[n]$ with edge weights $w_{ij} = \|x_i - x_j\| \mathbb{I}\{\|x_i - x_j\| \leq r\}$

2: compute the shortest-path distances in that graph $\Gamma = (\gamma_{ij})$

3: apply classical scaling with inputs $\Gamma^{\circ 2}$ and d , resulting in points $y_1, \dots, y_n \in \mathbb{R}^d$

Return: the points y_1, \dots, y_n

5.1 A performance bound for (Landmark) Isomap

Isomap is a well-known method for manifold learning, suggested by Tenenbaum, de Silva, and Langford [31]. Algorithm 4 describes the method. (There, we use the notation $A^{\circ 2}$ to denote the matrix with entries A_{ij}^2 .)

There are two main components to Isomap: 1) Form the r -ball neighborhood graph based on the data points and compute the shortest-path distances; 2) Pass the obtained distance matrix to classical scaling (together with the desired embedding dimension) to obtain an embedding. The algorithm is known to work well when the underlying manifold is isometric to a convex domain in \mathbb{R}^d . Indeed, assuming an infinite sample size, so that the data points are in fact all the points of the manifold, as $r \rightarrow 0$, the shortest-path distances will converge to the geodesic distances on the manifold, and thus, in that asymptote (infinite sample size and infinitesimal radius), an isometric embedding in \mathbb{R}^d is possible under the stated condition. We will assume that this condition, that the manifold is isometric to a convex subset of \mathbb{R}^d , holds.

In an effort to understand the performance of Isomap, Bernstein et al. [4] study how well the shortest-path distances in the r -ball neighborhood graph approximate the actual geodesic distances. Before stating their result we need to state a definition.

Definition 1. The *reach* of a subset \mathcal{A} in some Euclidean space is the supremum over $t \geq 0$ such that, for any point x at distance at most t from \mathcal{A} , there is a unique point among those belonging to \mathcal{A} that is closest to x . When \mathcal{A} is a C^2 submanifold, its reach is known to bound its radius of curvature from below [11].

Assume that the manifold \mathcal{M} has reach at least $\tau > 0$, and the data points are sufficiently dense in that

$$\min_{i \in [n]} g_{\mathcal{M}}(x, x_i) \leq a, \quad \forall x \in \mathcal{M}, \quad (23)$$

where $g_{\mathcal{M}}$ denote the metric on \mathcal{M} (induced by the surrounding Euclidean metric). If r is sufficiently small in that $r < \tau$, then Bernstein et al. [4] show that

$$1 - c_0(r/\tau)^2 \leq \frac{\gamma_{ij}}{g_{ij}} \leq 1 + c_0(a/r), \quad \forall i, j \in [n], \quad (24)$$

where γ_{ij} is the graph distance, g_{ij} is the geodesic distance between x_i and x_j , and $c_0 \geq 1$ is a universal constant. (In fact, Bernstein et al. [4] derive such a bound under the additional condition that \mathcal{M} is geodesically convex, although the result can be generalized without much effort [1].)

We are able to improve the upper bound in the restricted setting considered here, where the underlying manifold is assumed to be isometric to a convex domain.

Proposition 1. *In the present situation, there is a universal constant $c_1 \geq 1$ such that, if $a/r \leq 1/\sqrt{c_1}$,*

$$\frac{\gamma_{ij}}{g_{ij}} \leq 1 + c_1(a/r)^2, \quad \forall i, j \in [n]. \quad (25)$$

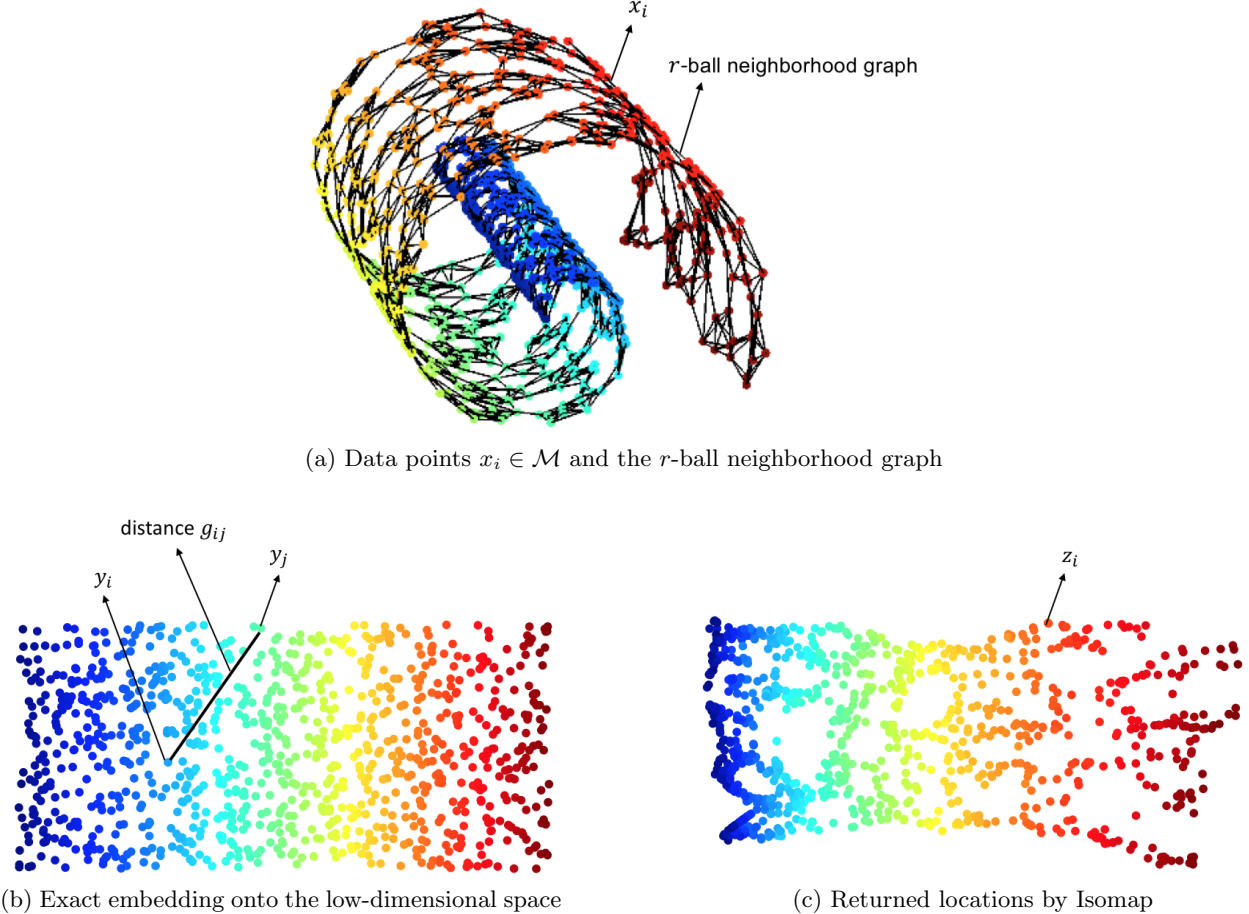


Figure 1: Schematic representation of exact locations $y_i \in \mathbb{R}^d$, data points $x_i \in \mathcal{M}$, returned locations by Isomap $z_i \in \mathbb{R}^d$. Note that $g_{ij} = \|y_i - y_j\|$ is the geodesic distance between x_i and x_j because $\{y_i\}_{i=1}^n$ is an exact isometric embedding of data points $\{x_i\}_{i=1}^n$. Also the distances γ_{ij} are computed as shortest path distances between x_i and x_j on the r -ball neighborhood graph.

Thus, if we set $\xi = c_0(r/\tau)^2 \vee c_1(a/r)^2$, and it happens that $\xi < 1$, we have

$$1 - \xi \leq \frac{\gamma_{ij}}{g_{ij}} \leq 1 + \xi, \quad \forall i, j \in [n]. \quad (26)$$

Armed with our perturbation bound for classical scaling, we are able to complete the analysis of Isomap, obtaining the following performance bound.

Corollary 3. *In the present context, let $y_1, \dots, y_n \in \mathbb{R}^d$ denote a possible (exact and centered) embedding of the data points $x_1, \dots, x_n \in \mathcal{M}$, and let ρ and ω denote the max-radius and half-width of the embedded points, respectively. If $\xi \leq \frac{1}{12}(\rho/\omega)^{-3}$, then Isomap returns $z_1, \dots, z_n \in \mathbb{R}^d$ satisfying*

$$\min_{Q \in \mathcal{O}} \left(\frac{1}{n} \sum_{i \in [n]} \|z_i - Qy_i\|^2 \right)^{1/2} \leq \frac{24\sqrt{d}\rho^3}{\omega^2} \xi. \quad (27)$$

Proof. Before we provide the proof, we refer to Figure 1 for a schematic representation of exact locations $y_i \in \mathbb{R}^d$, data points $x_i \in \mathcal{M}$, returned locations by Isomap $z_i \in \mathbb{R}^d$, as well as graph distances γ_{ij} and geodesic distances g_{ij} .

The proof itself is a simple consequence of Corollary 1. Indeed, with (26) it is straightforward to obtain (with η defined in Corollary 1 and γ_{ij} and g_{ij} as above),

$$\eta^2 \leq \max_{i,j \in [n]} |\gamma_{ij}^2 - g_{ij}^2| \leq \max_{i,j \in [n]} (2\xi + \xi^2) g_{ij}^2 \leq (2\xi + \xi^2)(2\rho)^2 \leq 12\rho^2\xi, \quad (28)$$

using the fact that $\xi \leq 1$ by the assumed upper bound (and the fact that $\omega \leq \rho$). In particular, η fulfills the conditions of Corollary 1 under the stated bound ξ , so we may conclude by applying that corollary and simplifying. \square

If \mathcal{D} is a domain in \mathbb{R}^d that is isometric to \mathcal{M} , then the radius of the embedded points (ρ above) can be bounded from above by the radius of \mathcal{D} , and under mild assumptions on the sampling, the half-width of the embedded points (ω above) can be bounded from below by a constant times the half-width of \mathcal{D} , in which case ρ and ω should be regarded as fixed. Similarly, τ should be considered as fixed, so that the bound is of order $O(r^2 \vee (a/r)^2)$, optimized at $r \asymp a^{1/2}$. If the points are well spread-out, for example if the points are sampled iid from the uniform distribution on the manifold, then a is on the order of $(\log(n)/n)^{1/d}$, and the bound (with optimal choice of radius) is in $O(\log(n)/n)^{1/d}$.

Landmark Isomap Because of the relatively high computational complexity of Isomap, and also of classical scaling, de Silva and Tenenbaum [7, 8] proposed a Nyström approximation (as explained in [23]). Seen as a method for MDS, it starts by embedding a small number of items, which effectively play the role of landmarks, and then embedding the remaining items by trilateration based on these landmarks. Seen as a method for manifold learning, the items are the points in space, and the dissimilarities are the squared graph distances, which are not provided and need to be computed. Algorithm 5 details the method in this context. The landmarks may be chosen at random from the data points, although other options are available, and we discuss some of them in Section 6.2.

Algorithm 5 Landmark Isomap

Input: data points $x_1, \dots, x_n \in \mathbb{R}^D$, embedding dimension d , neighborhood radius r , number of landmarks ℓ

Output: embedding points $y_1, \dots, y_n \in \mathbb{R}^d$

1: construct the graph on $[n]$ with edge weights $w_{ij} = \|x_i - x_j\| \mathbb{I}\{\|x_i - x_j\| \leq r\}$

2: select $\mathcal{L} \subset [n]$ of size ℓ according to one of the methods in Section 6.2

3: compute the shortest-path distances in that graph $\Gamma = (\gamma_{ij})$ for $(i, j) \in [n] \times \mathcal{L}$

4: apply classical scaling with inputs $\Gamma_{\mathcal{L} \times \mathcal{L}}^{\circ 2}$ and d , resulting in (landmark) points $y_i, i \in \mathcal{L}$ in \mathbb{R}^d

5: for each $i \notin \mathcal{L}$, apply trilateration based on $\{y_j : j \in \mathcal{L}\}$ and $\Gamma_{i \times \mathcal{L}}^{\circ 2}$ to obtaining $y_i \in \mathbb{R}^d$

Return: the points y_1, \dots, y_n

With our work, we are able to provide a performance bound for Landmark Isomap.

Corollary 4. *In the same context as in Corollary 3, if one uses a set \mathcal{L} of $\ell \leq n/2$ landmarks with embedded half-width $\omega_* > 0$, and $\xi \leq (36\sqrt{d\ell})^{-1}(\rho/\omega_*)^{-3}$, then Landmark Isomap returns $z_1, \dots, z_n \in \mathbb{R}^d$ satisfying*

$$\min_{Q \in \mathcal{O}} \left(\frac{1}{n} \sum_{i \in [n]} \|z_i - Qy_i\|^2 \right)^{1/2} \leq C_1 \frac{\sqrt{d}\rho^5}{\omega_*^4} \sqrt{\ell}\xi, \quad (29)$$

where C_1 is a universal constant.

The result is a direct consequence of applying Corollary 3, which allows us to control the accuracy of embedding the landmarks using classical scaling, followed by applying Corollary 2, which allows us to control the accuracy of embedding using trilateration. The proof is given in Section 7.6.

We note that for the set of (embedded) landmarks to have positive half-width, it is necessary that they span the whole space, which compels $\ell \geq d + 1$. In Section 6.2 we show that choosing the landmarks at random performs reasonably well in that, with probability approaching 1 very quickly as ℓ increases, their (embedded) half-width is at least half that of the entire (embedded) point set.

5.2 A performance bound for Maximum Variance Unfolding

Maximum Variance Unfolding is another well-known method for manifold learning, proposed by Weinberger and Saul [37, 38]. Algorithm 6 describes the method, which relies on solving a semidefinite relaxation.

Algorithm 6 Maximum Variance Unfolding (MVU)

Input: data points $x_1, \dots, x_n \in \mathbb{R}^D$, embedding dimension d , neighborhood radius r
Output: embedding points $y_1, \dots, y_n \in \mathbb{R}^d$

- 1: set $\gamma_{ij} = \|x_i - x_j\|$ if $\|x_i - x_j\| \leq r$, and $\gamma_{ij} = \infty$ otherwise
- 2: solve the following semidefinite program

$$\text{maximize} \sum_{i,j \in [n]} \|z_i - z_j\|^2 \text{ over } z_1, \dots, z_n \in \mathbb{R}^d, \text{ subject to } \|z_i - z_j\| \leq \gamma_{ij} \quad (30)$$

- 3: center a solution set and embed it using principal component analysis

Return: the embed point set, denoted by y_1, \dots, y_n

Although MVU is broadly regarded to be more stable than Isomap, Arias-Castro and Pelletier [2] show that it works as intended under the same conditions required by Isomap, namely, that the underlying manifold is geodesically convex. Under these conditions, in fact, under the same conditions as in Corollary 3, where in particular (26) is assumed to hold with ξ sufficiently small, Paprotny and Gärcke [22] show that MVU returns an embedding, $z_1, \dots, z_n \in \mathbb{R}^d$, with dissimilarity matrix $\Lambda = (\gamma_{ij})$, $\gamma_{ij} = \|z_i - z_j\|^2$, satisfying

$$|\Lambda - \Delta|_1 \leq 9\rho^2 n^2 \xi, \quad (31)$$

where $\Delta = (\delta_{ij})$, $\delta_{ij} = \|y_i - y_j\|^2$ (the correct underlying distances), and for a matrix $A = (a_{ij})$, $|A|_p^p = \sum_{i,j} |a_{ij}|^p$. Based on that, and on our work in Section 3, we are able to provide the following performance bound for MVU, which is morally identical to the bound we obtained for Isomap.

Corollary 5. *In the same context as in Corollary 3, if instead $\xi \leq (6\sqrt{3}\sqrt{d})^{-1}(\rho/\omega)^{-3}$, then Maximum Variance Unfolding returns $z_1, \dots, z_n \in \mathbb{R}^d$ satisfying*

$$\min_{Q \in \mathcal{O}} \left(\frac{1}{n} \sum_{i \in [n]} \|z_i - Qy_i\|^2 \right)^{1/2} \leq \frac{12\sqrt{3}\sqrt{d}\rho^3}{\omega^2} \xi. \quad (32)$$

Proof. As in (28), we have

$$|\Lambda - \Delta|_\infty = \max_{i,j \in [n]} |\gamma_{ij}^2 - g_{ij}^2| \leq 12\rho^2 \xi, \quad (33)$$

so that, in combination with (31), we have

$$\|\Lambda - \Delta\|_2 \leq |\Lambda - \Delta|_\infty^{1/2} |\Lambda - \Delta|_1^{1/2} \leq 6\sqrt{3}n\rho^2\xi. \quad (34)$$

In particular, the conditions of Corollary 1 are met under the stated bound on ξ . Therefore, we may apply that corollary to conclude. \square

6 Discussion

6.1 Optimality considerations

The performance bounds that we derive for Isomap and Maximum Variance Unfolding are the same up to a universal multiplicative constant. This may not be surprising as they are known to be closely related, since the work of Paprotny and Gacke [22]. Based on our analysis of classical scaling, we believe that the bound for Isomap is sharp up to a multiplicative constant. But one may wonder if Maximum Variance Unfolding, or a totally different method, can do strictly better.

This optimality problem can be formalized as follows:

Consider the class of isometries $\varphi : \mathcal{D} \rightarrow \mathcal{M} \subset \mathbb{R}^D$, one-to-one, such that its domain \mathcal{D} is a convex subset of \mathbb{R}^d with max-radius at most ρ_0 and half-width at least $\omega_0 > 0$, and its range \mathcal{M} is a submanifold with reach at least $\tau_0 > 0$. To each such isometry φ , we associate the uniform distribution on its range \mathcal{M} , denoted by P_φ . We then assume that we are provided with iid samples of size n from P_φ , for some unknown isometry φ in that class. If the sample is denoted by $x_1, \dots, x_n \in \mathcal{M}$, with $x_i = \varphi(y_i)$ for some $y_i \in \mathcal{D}$, the goal is to recover y_1, \dots, y_n up to a rigid transformation, and the performance is measured in average squared error. Then, what is the optimal achievable performance?

Despite some closely related work on manifold estimation, in particular work of Genovese et al. [12] and of Kim and Zhou [19], we believe the problem remains open. Indeed, while in the setting in dimension $d = 1$ the two problems are particularly close, in dimension $d \geq 2$ the situation here appears more delicate here, as it relies on a good understanding of the interpolation of points by isometries.

6.2 Choosing landmarks

In this subsection we discuss the choice of landmarks. We consider the two methods originally proposed by de Silva and Tenenbaum [8]:

- **Random.** The landmarks are chosen uniformly at random from the data points.
- **MaxMin.** After choosing the first landmark uniformly at random from the data points, each new landmark is iteratively chosen from the data points to maximize the minimum distance to the existing landmarks.

(For both methods, de Silva and Tenenbaum [8] recommend using different initializations.)

The first method is obviously less computationally intensive compared to the second method, but the hope in the more careful (and also more costly) selection of landmarks in the second method is that it would require fewer landmarks to be selected. In any case, de Silva and Tenenbaum [8] observe that the random selection is typically good enough in practice, so we content ourselves with analyzing this method.

In view of our findings (Corollary 2), a good choice of landmarks is one that has large (embedded) half-width, ideally comparable to, or even larger than that of the entire dataset. In that light, the

problem of selecting good landmarks is closely related, if not identical, to problem of selecting rows of a tall matrix in a way that leads to a submatrix with good condition number. In particular, several papers have established bounds for various ways of selecting the rows, some of them listed in [16, Tab 2]. Here the situation is a little different in that the dissimilarity matrix is not directly available, but rather, rows (corresponding to landmarks) are revealed as they are selected.

The **Random** method, nonetheless, has been studied in the literature. Rather than fetch existing results, we provide a proof for the sake of completeness. As everyone else, we use random matrix concentration [33]. We establish a bound for a slightly different variant where the landmarks are selected with replacement, as it simplifies the analysis. Related work is summarized in [16, Tab 3], although for the special case where the data matrix (denoted Y earlier) has orthonormal columns (an example of paper working in this setting is [17]).

Proposition 2. *Suppose we select ℓ landmarks among n points in dimension d , with half-width ω and max-radius ρ_∞ , according to the **Random** method, but with replacement. Then with probability at least $1 - 2(d+1) \exp[-\ell\omega^2/9\rho_\infty^2]$, the half-width of the selected landmarks is at least $\omega/2$.*

The proof of Proposition 2 is given in Section A.3. Thus, if $\ell \geq 9(\rho_\infty/\omega)^2 \log(2(d+1)/\delta)$, then with probability at least $1 - \delta$ the landmark set has half-width at least $\omega/2$. Consequently, if the dataset is relatively well-conditioned in that its aspect ratio, ρ_∞/ω , is relatively small, then **Random** (with replacement) only requires the selection of a few landmarks in order to output a well-conditioned subset (with high probability).

7 Proofs

7.1 Preliminaries

We start by stating a number of lemmas pertaining to linear algebra and end the section with a result for a form of procrustes analysis, a well-known method for matching two sets of points in a Euclidean space.

Schatten norms For a matrix² A , we let $\nu_1(A) \geq \nu_2(A) \geq \dots$ denote its singular values. Let $\|\cdot\|_p$ denote the following Schatten quasi-norm,

$$\|A\|_p \equiv (\nu_1(A)^p + \dots + \nu_d(A)^p)^{1/p}, \quad (35)$$

which is a true norm when $p \in [1, \infty]$. When $p = 2$ it corresponds to the Frobenius norm (which will also be denoted by $\|\cdot\|_2$) and when $p = \infty$ it corresponds to the usual operator norm (which will also be denoted by $\|\cdot\|$). We mention that each Schatten quasi-norm is unitary invariant, and satisfies

$$\|AB\|_p \leq \|A\|_\infty \|B\|_p, \quad (36)$$

any matrices of compatible sizes, and it is sub-multiplicative if it is a norm ($p \geq 1$). In addition, $\|A\|_p = \|A^\top\|_p$ and $\|A\|_p = \|A^\top A\|_{p/2}^{1/2} = \|AA^\top\|_{p/2}^{1/2}$, due to the fact that

$$\|A\|_p^p = \sum_j \nu_j(A)^p = \sum_j \nu_j(A^\top A)^{p/2} = \|A^\top A\|_{p/2}^{p/2}, \quad (37)$$

and if A and B are positive semidefinite satisfying $A \preceq B$, where \preceq denotes the Loewner order, then $\|A\|_p \leq \|B\|_p$, due to the fact that $\nu_j(A) \leq \nu_j(B)$ for all j in that case. Unless otherwise

² All the matrices and vectors we consider are real, unless otherwise specified.

specified, p will be fixed in $[1, \infty]$. Note that, for any fixed matrix A , $\|A\|_p \leq \|A\|_q$ whenever $q \leq p$, and

$$\|A\|_p \rightarrow \|A\|_\infty, \quad p \rightarrow \infty. \quad (38)$$

Moore-Penrose pseudo-inverse The Moore-Penrose pseudo-inverse of a matrix is defined as follows [30, Thm III.1]. Let A be a m -by- k matrix, where $m \geq k$, with singular value decomposition $A = UDV^\top$, where U is m -by- k orthogonal, V is k -by- k orthogonal, and D is k -by- k diagonal with diagonal entries $\nu_1 \geq \dots \geq \nu_l > 0 = \dots = 0$, so that the ν_j 's are the nonzero singular values of A and A has rank l . The pseudo-inverse of A is defined as $A^\ddagger = VD^\ddagger U^\top$, where $D^\ddagger = \text{diag}(\nu_1^{-1}, \dots, \nu_l^{-1}, 0, \dots, 0)$. If the matrix A is tall and full rank, then $A^\ddagger = (A^\top A)^{-1} A^\top$. In particular, if a matrix is square and non-singular, its pseudo-inverse coincides with its inverse.

Lemma 1. *Suppose that A is a tall matrix with full rank. Then A^\ddagger is non-singular, and for any other matrix B of compatible size,*

$$\|B\|_p \leq \|A^\ddagger\|_\infty \|AB\|_p. \quad (39)$$

Proof. This simply comes from the fact that $A^\ddagger A = I$ (since A is tall and full rank), so that

$$\|B\|_p = \|A^\ddagger AB\|_p \leq \|A^\ddagger\|_\infty \|AB\|_p, \quad (40)$$

by (36). \square

Lemma 2. *Let A and B be matrices of same size. Then, for $p \in \{2, \infty\}$,*

$$\|B^\ddagger - A^\ddagger\|_p \leq \frac{\sqrt{2} \|A^\ddagger\|^2 \|B - A\|_p}{(1 - \|A^\ddagger\| \|B - A\|)_+^2}. \quad (41)$$

Proof. A result of Wedin [30, Thm III.3.8] gives

$$\|B^\ddagger - A^\ddagger\|_p \leq \sqrt{2} (\|B^\ddagger\| \vee \|A^\ddagger\|)^2 \|B - A\|_p, \quad p \in \{2, \infty\}. \quad (42)$$

Assuming B has exactly k nonzero singular values, using Mirksky's inequality [30, Thm IV.4.11], namely

$$\max_j |\nu_j(B) - \nu_j(A)| \leq \|B - A\|, \quad (43)$$

we have

$$\|B^\ddagger\|^{-1} = \nu_k(B) \geq (\nu_k(A) - \|B - A\|)_+ \geq (\|A^\ddagger\|^{-1} - \|B - A\|)_+. \quad (44)$$

By combining Equations (42) and (44), we get

$$\|B^\ddagger - A^\ddagger\|_p \leq \sqrt{2} \left(\|A^\ddagger\| \vee \frac{1}{(\|A^\ddagger\|^{-1} - \|B - A\|)_+} \right)^2 \|B - A\|_p, \quad (45)$$

from which the result follows. \square

Some elementary matrix inequalities The following lemmas are elementary inequalities involving Schatten norms.

Lemma 3. *For any two matrices A and B of same size such that $A^\top B = 0$ or $AB^\top = 0$,*

$$\|A + B\|_p \geq \|A\|_p \vee \|B\|_p. \quad (46)$$

Proof. Assume without loss of generality that $A^\top B = 0$. In that case, $(A + B)^\top(A + B) = A^\top A + B^\top B$, which is not smaller than $A^\top A$ or $B^\top B$ in the Loewner order. Therefore,

$$\|A\|_p = \|A^\top A\|_{p/2}^{1/2} \leq \|A^\top A + B^\top B\|_{p/2}^{1/2} \quad (47)$$

$$= \|(A + B)^\top(A + B)\|_{p/2}^{1/2} = \|A + B\|_p, \quad (48)$$

applying several of the properties listed above for Schatten (quasi)norms. \square

Lemma 4. *For any positive semidefinite matrix A ,*

$$\|A - I\|_p \leq \|A^2 - I\|_p, \quad (49)$$

where I denotes the identity matrix.

Proof. By the spectral theorem, we may diagonalize A , which reduces the situation where A is diagonal, $A = \text{diag}(a_1, a_2, \dots)$, say, with $a_1 \geq a_2 \geq \dots \geq 0$, since a Schatten norm is unitary invariant. Assuming $p < \infty$, we have

$$\|A - I\|_p^p = \sum_j |a_j - 1|^p \leq \sum_j |a_j - 1|^p (a_j + 1)^p = \sum_j |a_j^2 - 1|^p = \|A^2 - I\|_p^p. \quad (50)$$

The case where $p = \infty$ can be solved similarly, or by continuity based on (38). \square

7.2 Proof of Theorem 1

Let P be the orthogonal projection onto the range of X , which can be expressed as $P = XX^\dagger$. Define $Y_1 = PY$ and $Y_2 = (I - P)Y$, and note that $Y = Y_1 + Y_2$ with $Y_2^\top Y_1 = 0$, and also $Y_2^\top X = 0$.

Define $M = X^\dagger Y$, and apply a singular value decomposition to obtain $M = UDV^\top$, where U and V are orthogonal, and D is diagonal with nonnegative entries. Then define $Q = UV^\top$, which is orthogonal. We show that the bound (4) holds for this orthogonal matrix.

We start with the triangle inequality,

$$\|Y - XQ\|_p = \|Y_1 - XQ + Y_2\|_p \leq \|Y_1 - XQ\|_p + \|Y_2\|_p.$$

Noting that $Y_1 = XX^\dagger Y = XM$, we have

$$\begin{aligned} \|Y_1 - XQ\|_p &= \|XM - XQ\|_p = \|XUDV^\top - XUV^\top\|_p \\ &= \|XU(D - I)V^\top\|_p \leq \|X\| \|D - I\|_p, \end{aligned}$$

using (36) and unitary invariance. By (49), we have

$$\|D - I\|_p \leq \|D^2 - I\|_p = \|MM^\top - I\|_p, \quad (51)$$

and, by (36),

$$\begin{aligned}\|MM^\top - I\|_p &= \|X^\dagger X(MM^\top - I)(X^\dagger X)^\top\|_p \\ &\leq \|X^\dagger\|^2 \|X(MM^\top - I)X^\top\|_p \\ &= \|X^\dagger\|^2 \|XMM^\top X^\top - XX^\top\|_p \\ &= \|X^\dagger\|^2 \|Y_1 Y_1^\top - XX^\top\|_p.\end{aligned}$$

Coming from the other end, so to speak, we have

$$\varepsilon^2 = \|YY^\top - XX^\top\|_p = \|Y_1 Y_1^\top - XX^\top + Y_1 Y_2^\top + Y_2 Y_1^\top + Y_2 Y_2^\top\|_p \quad (52)$$

$$\geq \|Y_1 Y_1^\top - XX^\top + Y_1 Y_2^\top\| \vee \|Y_2 Y_1^\top + Y_2 Y_2^\top\|_p \quad (53)$$

$$\geq \|Y_1 Y_1^\top - XX^\top\|_p \vee \|Y_1 Y_2^\top\|_p \vee \|Y_2 Y_1^\top\|_p \vee \|Y_2 Y_2^\top\|_p, \quad (54)$$

using Lemma 3 thrice, once based on the fact that

$$(Y_1 Y_1^\top - XX^\top + Y_1 Y_2^\top)^\top (Y_2 Y_1^\top + Y_2 Y_2^\top) = \underbrace{(Y_1 Y_1^\top - XX^\top + Y_2 Y_1^\top) Y_2 (Y_1^\top + Y_2^\top)}_{=0} = 0,$$

and then based on the fact that

$$(Y_1 Y_1^\top - XX^\top) (Y_1 Y_2^\top)^\top = \underbrace{(Y_1 Y_1^\top - XX^\top) Y_2}_{=0} Y_1^\top = 0,$$

and

$$(Y_2 Y_1^\top) (Y_2 Y_2^\top)^\top = Y_2 \underbrace{Y_1^\top Y_2}_{=0} Y_2^\top.$$

From (54), we extract the bound $\|Y_1 Y_1^\top - XX^\top\|_p \leq \varepsilon^2$, from which we get (based on the derivations above)

$$\|Y_1 - XQ\|_p \leq \|X\| \|X^\dagger\|^2 \varepsilon^2. \quad (55)$$

From (54), we extract the bound $\|Y_1 Y_2^\top\|_p \leq \varepsilon^2$, and combine it with

$$\begin{aligned}\|Y_1 Y_2^\top\|_p &\geq \|XQ Y_2^\top\|_p - \|(Y_1 - XQ) Y_2^\top\|_p \\ &\geq (\|(XQ)^\dagger\|^{-1} - \|Y_1 - XQ\|_p) \|Y_2^\top\|_p \\ &= (\|X^\dagger\|^{-1} - \|X\| \|X^\dagger\|^2 \varepsilon^2) \|Y_2\|_p,\end{aligned}$$

using the triangle inequality, (39) (which is applicable since XQ has full rank), and (55), to get

$$\|Y_2\|_p \leq (1 - \|X\| \|X^\dagger\|^3 \varepsilon^2)^{-1} \|X^\dagger\| \varepsilon^2, \quad (56)$$

where the right-hand side is bounded by $2 \|X^\dagger\| \varepsilon^2$ when $\|X^\dagger\| \varepsilon \leq \frac{1}{\sqrt{2}} (\|X\| \|X^\dagger\|)^{-1}$.

From this we establish the announced result, namely (4) under the stated conditions. Yet from (54), we can also extract the bound $\|Y_2 Y_2^\top\|_p \leq \varepsilon^2$, and combine it with

$$\|Y_2 Y_2^\top\|_p = \|Y_2\|_{2p}^2 \geq d^{-1/p} \|Y_2\|_p^2,$$

where d is the number of columns and the inequality is Cauchy-Schwarz's, to get

$$\|Y_2\|_p \leq d^{1/2p} \varepsilon,$$

and combining these bounds, we get

$$\|Y - XQ\|_p \leq \|X\| \|X^\dagger\|^2 \varepsilon^2 + (1 - \|X\| \|X^\dagger\|^3 \varepsilon^2)^{-1} \|X^\dagger\| \varepsilon^2 \wedge d^{1/2p} \varepsilon, \quad (57)$$

which is somewhat sharper than (4).

7.3 Proof of Theorem 3

Let \bar{a} denote the average dissimilarity vector defined in Algorithm 3 based on Y , and define \bar{b} similarly based on Z . Let Λ denote the matrix of dissimilarities between X and Z , and let \hat{X} denote the result of Algorithm 3 with inputs Z and Λ . From Algorithm 3, we have

$$X^\top = \frac{1}{2}Y^\ddagger(\bar{a}1^\top - \Delta^\top), \quad \hat{X}^\top = \frac{1}{2}Z^\ddagger(\bar{b}1^\top - \Lambda^\top), \quad \tilde{X}^\top = \frac{1}{2}Z^\ddagger(\bar{b}1^\top - \Theta^\top), \quad (58)$$

due to the fact that the algorithm is exact.

We have

$$\|\tilde{X} - X\|_2 \leq \|\tilde{X} - \hat{X}\|_2 + \|\hat{X} - X\|_2. \quad (59)$$

On the one hand,

$$2\|\tilde{X} - \hat{X}\|_2 \leq \|Z^\ddagger\|\|\Theta - \Lambda\|_2 \leq \|Z^\ddagger\|(\|\Theta - \Delta\|_2 + \|\Delta - \Lambda\|_2). \quad (60)$$

On the other hand, starting with the triangle inequality,

$$\begin{aligned} 2\|\hat{X} - X\|_2 &= \|Z^\ddagger(\bar{b}1^\top - \Lambda^\top) - Y^\ddagger(\bar{a}1^\top - \Delta^\top)\|_2 \\ &\leq \|Z^\ddagger(\bar{b}1^\top - \Lambda^\top) - Z^\ddagger(\bar{a}1^\top - \Delta^\top)\|_2 + \|Z^\ddagger(\bar{a}1^\top - \Delta^\top) - Y^\ddagger(\bar{a}1^\top - \Delta^\top)\|_2 \\ &\leq \|Z^\ddagger\|(\|\bar{b}1^\top - \bar{a}1^\top\|_2 + \|\Lambda - \Delta\|_2) + \|\bar{a}1^\top - \Delta^\top\| \|Z^\ddagger - Y^\ddagger\|_2. \end{aligned}$$

Together, we find that

$$2\|\tilde{X} - X\|_2 \leq \|Z^\ddagger\|(\|\Theta - \Delta\|_2 + 2\|\Lambda - \Delta\|_2 + \sqrt{m}\|\bar{b} - \bar{a}\|) + \|\bar{a}1^\top - \Delta^\top\| \|Z^\ddagger - Y^\ddagger\|_2. \quad (61)$$

In the following, we bound the terms $\|\bar{a}1^\top - \Delta^\top\|$, $\|\Lambda - \Delta\|_2$ and $\|\bar{b} - \bar{a}\|$, separately. First, using Lemma 1 and the fact that $(Y^\ddagger)^\ddagger = Y$ has full rank,

$$\|X\| = \frac{1}{2}\|Y^\ddagger(\bar{a}1^\top - \Delta^\top)\| \geq \frac{1}{2}\|Y\|^{-1}\|\bar{a}1^\top - \Delta^\top\|. \quad (62)$$

Therefore,

$$\|\bar{a}1^\top - \Delta^\top\| \leq 2\|Y\|\|X\|. \quad (63)$$

Next, set $Y = [y_1 \cdots y_m]^\top$ and $Z = [z_1 \cdots z_m]^\top$, as well as $X = [x_1 \cdots x_n]^\top$. Since

$$(\Lambda - \Delta)_{ij} = 2x_i^\top(y_j - z_j) + \|z_j\|^2 - \|y_j\|^2, \quad (64)$$

we have

$$\|\Lambda - \Delta\|_2 = \|2X(Y^\top - Z^\top) + 1c^\top\|_2 \leq 2\|X\|\|Y - Z\|_2 + \sqrt{m}\|c\|, \quad (65)$$

with $c = (c_1, \dots, c_m)$ and $c_j = \|z_j\|^2 - \|y_j\|^2$. Note that

$$\begin{aligned} \|c\|^2 &= \sum_{j \in [m]} (\|z_j\|^2 - \|y_j\|^2)^2 \\ &\leq \sum_{j \in [m]} \|z_j - y_j\|^2 (\|z_j\| + \|y_j\|)^2 \\ &\leq (\rho_\infty(Y) + \rho_\infty(Z))^2 \|Z - Y\|_2^2, \end{aligned}$$

so that

$$\|\Lambda - \Delta\|_2 \leq 2\|X\|\|Y - Z\|_2 + \sqrt{m}(\rho_\infty(Y) + \rho_\infty(Z))\|Z - Y\|_2. \quad (66)$$

Finally, recall that \bar{a} and \bar{b} are respectively the average of the columns of the dissimilarity matrix for the landmark Y and the landmark Z . Using the fact that the y 's are centered and that the z 's are also centered, we get

$$\bar{b} - \bar{a} = c - \bar{c}1, \quad (67)$$

where $\bar{c} = \frac{1}{m} \sum_{j \in [m]} c_j$, so that

$$\|\bar{b} - \bar{a}\|^2 \leq \sum_{j \in [m]} (c_j - \bar{c})^2 = \|c\|^2 - m\bar{c}^2 \leq \|c\|^2. \quad (68)$$

Combining all these bounds, we obtain the bound stated in (19). The last part comes from the triangle inequality and an application of Lemma 2.

7.4 Proof of Corollary 1

We apply Theorem 2 with $p = \infty$. Using (36) and the fact that $\|H\|_\infty$ (since H is an orthogonal projection), we have

$$2\varepsilon^2 = \|H(\Lambda - \Delta)H\| \leq \|\Lambda - \Delta\| \leq \|\Lambda - \Delta\|_2 = m\eta^2 \leq m\omega^2(\rho/\omega)^{-1}. \quad (69)$$

Therefore

$$\|Y^\ddagger\|\varepsilon = \frac{\varepsilon}{\sqrt{m}\omega} \leq \frac{1}{\sqrt{2}}(\rho/\omega)^{-1/2} = \frac{1}{\sqrt{2}}(\|Y\|\|Y^\ddagger\|)^{-1/2}. \quad (70)$$

Hence, by using Theorem 2 we have

$$\begin{aligned} \min_{Q \in \mathcal{O}} \left(\frac{1}{m} \sum_{i \in [m]} \|z_i - Qy_i\|^2 \right)^{1/2} &\leq \sqrt{\frac{d}{m}} \min_{Q \in \mathcal{O}} \|Z - YQ\| \\ &\leq \sqrt{\frac{d}{m}}(\rho/\omega + 2) \frac{\varepsilon^2}{\sqrt{m}\omega} \\ &\leq \sqrt{d}(\rho/\omega + 2) \frac{\eta^2}{2\omega} \leq \frac{2\sqrt{d}\rho\eta^2}{\omega^2}, \end{aligned} \quad (71)$$

where the penultimate inequality follows from (69) and the last inequality holds since $\omega \leq \rho$.

7.5 Proof of Corollary 2

We apply Theorem 3 to $X = [x_1 \cdots x_n]^\top$, $Y = [y_1 \cdots y_m]^\top$, and $Z = [z_1 \cdots z_m]^\top$. To be in the same setting, we need Z to have full rank. As we point out in Remark 4, this is the case as soon as $\|Y^\ddagger\|\|Z - Y\| < 1$. Since $\|Y^\ddagger\| = (\sqrt{m}\omega)^{-1}$ and $\|Z - Y\| \leq \sqrt{m} \max_{i \in [m]} \|z_i - y_i\| \leq \sqrt{m}\varepsilon$, the condition is equivalent to $\varepsilon < \omega$, which is fulfilled by assumption. Continuing, we have

$$\|Z - Y\|_2 \leq \sqrt{m} \max_{i \in [m]} \|z_i - y_i\| \leq \sqrt{m}\varepsilon. \quad (72)$$

Hence, by (21),

$$\|Z^\ddagger - Y^\ddagger\|_2 \leq \frac{\frac{2}{m\omega^2}\sqrt{m}\varepsilon}{(1 - \frac{1}{\sqrt{m}\omega}\sqrt{m}\varepsilon)_+^2} \leq \frac{8\varepsilon}{\sqrt{m}\omega^2} \leq \frac{4}{\sqrt{m}\omega}, \quad (73)$$

using the fact that $\epsilon/\omega \leq 1/2$. Hence,

$$\|Z^\ddagger\| \leq \|Y^\ddagger\| + \|Z^\ddagger - Y^\ddagger\| \leq \frac{5}{\sqrt{m}\omega}, \quad (74)$$

Further, $\|\Delta - \Theta\|_2 = \sqrt{mn}\eta^2$. In addition, $\|X\| \leq \sqrt{n}\zeta$. Likewise, $\|Y\| \leq \sqrt{m}\rho$. Therefore, by applying Theorem 3, we get

$$\begin{aligned} \|\tilde{X} - X\|_2 &\leq \frac{5}{\sqrt{m}\omega} \left[\frac{1}{2} \sqrt{nm}\eta^2 + 2\sqrt{nm}\zeta\epsilon + \frac{3}{2} \sqrt{m}(2\rho_\infty + \epsilon)\sqrt{m}\epsilon \right] + (\sqrt{m}\rho)(\sqrt{n}\zeta) \frac{8\varepsilon}{\sqrt{m}\omega^2} \\ &\leq 30 \left(\frac{\sqrt{n}\eta^2}{\omega} + \frac{\sqrt{n}\zeta\epsilon}{\omega} + \frac{\rho_\infty + \epsilon}{\omega} \sqrt{m}\epsilon + \frac{\sqrt{n}\rho\zeta\varepsilon}{\omega^2} \right), \end{aligned} \quad (75)$$

from which we get the stated bound, using the fact that $\varepsilon \leq \omega \leq \rho \leq \rho_\infty$.

7.6 Proof of Corollary 4

Without loss of generality, suppose the chosen landmark points are x_1, \dots, x_ℓ . Using $\{\gamma_{ij} : i, j \in [\ell]\}$, we embed them using classical scaling, obtaining a centered point set $z_1, \dots, z_\ell \in \mathbb{R}^d$. By Corollary 3, which we may apply by our (stronger) assumption on ξ , we have

$$\min_{Q \in \mathcal{O}} \left(\frac{1}{\ell} \sum_{i \in [\ell]} \|z_i - Qy_i\|^2 \right)^{1/2} \leq \frac{24\sqrt{d}\rho_*^3}{\omega_*^2} \xi, \quad (76)$$

where ρ_* and ω_* are the max-radius and half-width of $\{y_i : i \in \mathcal{L}\}$. We may assume that the minimum above is attained at $Q = I$ without loss of generality, in which case we have

$$\varepsilon \equiv \max_{i \in [\ell]} \|z_i - y_i\| \leq \frac{24\sqrt{d}\rho^3}{\omega_*^2} \xi, \quad (77)$$

using the fact that $\rho_* \leq \rho$.

The next step consists in trilaterizing the remaining points based on the embedded landmarks. With η as in (28), and noting that $\varepsilon/\omega_* \leq 1/\sqrt{2}$ by our assumption on ξ , we may apply Corollary 2 (with the constant C_0 defined there) to obtain³

$$\frac{1}{C_0} \left(\frac{1}{n - \ell} \sum_{i=\ell+1}^n \|z_i - y_i\|^2 \right)^{1/2} \leq \frac{\eta^2}{\omega_*} + \left[\frac{\rho_*\rho}{\omega_*^2} + \frac{\sqrt{\ell}\rho_*}{\sqrt{n - \ell}\omega_*} \right] \varepsilon \quad (78)$$

$$\leq \frac{\eta^2}{\omega_*} + \frac{2\rho^2\varepsilon}{\omega_*^2} \quad (79)$$

$$\asymp \frac{\rho^2\xi}{\omega_*} + \frac{\rho^2}{\omega_*^2} \frac{\sqrt{d}\rho^3\xi}{\omega_*^2} \quad (80)$$

$$\asymp \frac{\sqrt{d}\rho^5}{\omega_*^4} \sqrt{\ell} \xi, \quad (81)$$

using the fact that $\omega_* \leq \rho_*$.

With this and the fact that

$$\left(\frac{1}{\ell} \sum_{i=1}^\ell \|z_i - y_i\|^2 \right)^{1/2} \leq \varepsilon, \quad (82)$$

and the bound on ε , we conclude.

³ In the present context, y_1, \dots, y_ℓ play the role of y_1, \dots, y_m ; $y_{\ell+1}, \dots, y_n$ play the role of x_1, \dots, x_n ; z_1, \dots, z_ℓ play the role of z_1, \dots, z_m ; and $z_{\ell+1}, \dots, z_n$ play the role of $\tilde{x}_1, \dots, \tilde{x}_n$.

Appendix

A.1 A succinct proof that Algorithm 3 is correct

To prove that Algorithm 3 is exact, it suffices to do so for the case where we want to position one point, i.e., when $n = 1$, and we denote that point by x . In that case, Δ is in fact a (row) vector, which we denote by δ^\top . We have $\|x - y_i\|^2 = \|x\|^2 + \|y_i\|^2 - 2y_i^\top x$, so that $\delta = \|x\|^2 1 + \zeta - 2Yx$, where $\zeta = (\|y_1\|^2, \dots, \|y_m\|^2)^\top$. We also have $\|y_j - y_i\|^2 = \|y_j\|^2 + \|y_i\|^2 - 2y_j^\top y_i$, so that $\bar{a} = a1 + \zeta$, where $a = \frac{1}{m}(\|y_1\|^2 + \dots + \|y_m\|^2)$, using the fact that $\frac{1}{m} \sum_{i=1}^m y_i = 0$. Hence, $\bar{a} - \delta = (a - \|x\|^2)1 + 2Yx$, and therefore,

$$\frac{1}{2}Y^\dagger(\bar{a} - \delta) = \frac{1}{2}(a - \|x\|^2)Y^\dagger 1 + Y^\dagger Yx. \quad (83)$$

We now use the fact that $Y^\dagger = (Y^\top Y)^{-1}Y^\top$. On the one hand, $Y^\dagger 1 = (Y^\top Y)^{-1}Y^\top 1 = 0$ since $Y^\top 1 = 0$ (because the point set is centered). On the other hand, $Y^\dagger Y = (Y^\top Y)^{-1}Y^\top Y = I$. We conclude that $\frac{1}{2}Y^\dagger(\bar{a} - \delta) = x$, which is what we needed to prove.

A.2 Proof of Proposition 1

The data points are denoted $x_1, \dots, x_n \in \mathcal{M}$, and by assumption we assume that $x_i = \varphi(y_i)$, where $\varphi : \mathcal{D} \rightarrow \mathcal{M}$ is a one-to-one isometry, with \mathcal{D} being a convex subset of \mathbb{R}^d . Fix $i, j \in [n]$, and note that $g_{ij} = g_{\mathcal{M}}(x_i, x_j) = \|y_i - y_j\|$.

If $g_{ij} \leq r$, then $\|x_i - x_j\| \leq g_{ij} \leq r$, so that i and j are neighbors in the graph, and in particular $\gamma_{ij} = \|x_i - x_j\|$. We may thus conclude that, in this situation, $\gamma_{ij} \leq g_{ij}$, which implies the stated bound.

Henceforth, we assume that $g_{ij} > r$. Consider $z_k = y_i + (k/m)(y_j - y_i)$, where $m = \lceil 2g_{ij}/r \rceil \geq 2$. Note that $z_0 = y_i$ and $z_m = y_j$. Let y_{i_k} be the closest point to z_k among $\{y_1, \dots, y_n\}$, with $i_0 = i$ and $i_m = j$. By the triangle inequality, we have

$$\|y_{i_{k+1}} - y_{i_k}\| \leq \|z_{k+1} - z_k\| + \|y_{i_{k+1}} - z_{k+1}\| + \|y_{i_k} - z_k\| \quad (84)$$

$$\leq \frac{1}{m}g_{ij} + 2a \leq r/2 + 2a \leq r, \quad (85)$$

if $a/r \leq 1/4$. Therefore,

$$\|x_{i_{k+1}} - x_{i_k}\| \leq g_{\mathcal{M}}(x_{i_{k+1}}, x_{i_k}) = \|y_{i_{k+1}} - y_{i_k}\| \leq r, \quad (86)$$

implying that $(i_k : k = 0, \dots, m)$ forms a path in the graph.

So far, the arguments are the same as in the proof of [4, Thm 2]. What makes our arguments sharper is the use of the Pythagoras theorem below. To make use of that theorem, we need to construct a different sequence of points on the line segment. Let \tilde{z}_k denote the orthogonal projection of y_{i_k} onto the line (denoted \mathcal{L}) defined by y_i and y_j . See Figure 2 for an illustration.

In particular the vector $\tilde{z}_k - y_{i_k}$ is orthogonal to \mathcal{L} , and

$$\|\tilde{z}_k - y_{i_k}\| = \min_{z \in \mathcal{L}} \|z - y_{i_k}\| \leq \|z_k - y_{i_k}\| \leq a. \quad (87)$$

It is not hard to see that \tilde{z}_k is in fact on the line segment defined by y_i and y_j . Moreover, they are

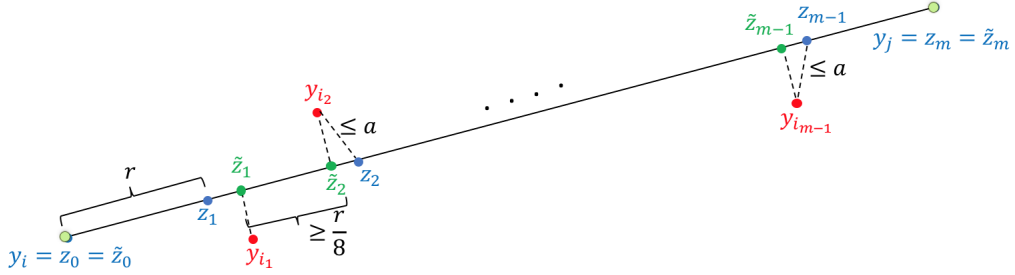


Figure 2: illustration for the proof of Proposition 1

located sequentially on that segment. Indeed, using the triangle inequality,

$$\|\tilde{z}_k - y_i\| \leq \|z_k - y_i\| + \|\tilde{z}_k - z_k\| \quad (88)$$

$$\leq \|z_k - y_i\| + \|z_k - y_{i_k}\| + \|y_{i_k} - \tilde{z}_k\| \quad (89)$$

$$\leq \|z_k - y_i\| + 2a \quad (90)$$

$$= \frac{k}{m}g_{ij} + 2a, \quad (91)$$

while, similarly,

$$\|\tilde{z}_{k+1} - y_i\| \geq \|z_{k+1} - y_i\| - 2a = \frac{k+1}{m}g_{ij} - 2a, \quad (92)$$

so that $\|\tilde{z}_k - y_i\| < \|\tilde{z}_{k+1} - y_i\|$ as soon as $g_{ij}/m > 4a$. Noting that $g_{ij} > (m-1)r/2$, this condition is met when $a/r \leq (m-1)/8m$. Recalling that $m \geq 2$, it is enough that $a/r \leq 1/16$. From the same derivations, we also get

$$\|\tilde{z}_{k+1} - \tilde{z}_k\| \geq \frac{1}{m}g_{ij} - 4a \geq \frac{(m-1)r}{2m} - 4a \geq r/8, \quad (93)$$

if $a/r \leq 1/32$.

Since $(i_k : k = 0, \dots, m)$ forms a path in the graph, we have

$$\gamma_{ij} \leq \sum_{k=0}^{m-1} \|x_{i_{k+1}} - x_{i_k}\| \leq \sum_{k=0}^{m-1} \|y_{i_{k+1}} - y_{i_k}\|. \quad (94)$$

By the Pythagoras theorem, we then have

$$\|y_{i_{k+1}} - y_{i_k}\|^2 = \|\tilde{z}_{k+1} - \tilde{z}_k\|^2 + \|y_{i_{k+1}} - \tilde{z}_{k+1} + \tilde{z}_k - y_{i_k}\|^2 \quad (95)$$

$$\leq \|\tilde{z}_{k+1} - \tilde{z}_k\|^2 + (2a)^2, \quad (96)$$

so that, using (93),

$$\|y_{i_{k+1}} - y_{i_k}\| \leq (1 + (2a)^2/(r/8)^2)^{1/2} \|\tilde{z}_{k+1} - \tilde{z}_k\| = (1 + C(a/r)^2) \|\tilde{z}_{k+1} - \tilde{z}_k\|, \quad (97)$$

where $C \leq 128$, yielding

$$\gamma_{ij} \leq (1 + C(a/r)^2) \sum_{k=0}^{m-1} \|\tilde{z}_{k+1} - \tilde{z}_k\| = (1 + C(a/r)^2) g_{ij}. \quad (98)$$

A.3 Proof of Proposition 2

We use concentration bounds for random matrices developed by Tropp [33]. Consider a point set $\mathcal{Y} = \{y_1, \dots, y_n\}$, assumed centered without loss of generality. We apply **Random** to select a subset of ℓ points chosen uniformly at random with replacement from \mathcal{Y} . We denote the resulting (random) point set by $\mathcal{Z} = \{z_1, \dots, z_\ell\}$. Let $Y = [y_1 \cdots y_n]$ and $Z = [z_1 \cdots z_\ell]$. We have that \mathcal{Y} has squared half-width equal to $\omega^2 \equiv \nu_d(Y^\top Y)/n$, and similarly, \mathcal{Z} has squared half-width equal to $\omega_Z^2 = \nu_d(Z^\top Z - \ell \bar{z} \bar{z}^\top)/\ell$, where $\bar{z} = (z_1 + \cdots + z_\ell)/\ell$. Note that, by (43),

$$\omega_Z^2 \geq \nu_d(Z^\top Z)/\ell - \nu_1(\bar{z} \bar{z}^\top) = \nu_d(Z^\top Z)/\ell - \nu_1(\bar{z})^2 = \nu_d(Z^\top Z)/\ell - \|\bar{z}\|^2. \quad (99)$$

We bound the two terms on the right-hand side separately.

First, we note that $Z^\top Z = \sum_j z_j z_j^\top$, with $z_1 z_1^\top, \dots, z_\ell z_\ell^\top$ sampled independently and uniformly from $\{y_1 y_1^\top, \dots, y_n y_n^\top\}$. These matrices are positive semidefinite, with expectation $Y^\top Y/n$, and have operator norm bounded by $\max_i \|y_i y_i^\top\| = \max_i \|y_i\|^2 = \rho_\infty^2$. We are thus in a position to apply [33, Thm 1.1, Rem 5.3], which gives that

$$\mathbb{P}\left(\nu_d(Z^\top Z)/\ell \leq \frac{1}{2}\omega^2\right) \leq d \exp\left[-\frac{1}{8}\ell\omega^2/\rho_\infty^2\right]. \quad (100)$$

Next, we note that $\ell \bar{z} = \sum_j z_j$, with z_1, \dots, z_n being iid uniform in $\{y_1, \dots, y_n\}$. These are here seen as rectangular $d \times 1$ matrices, with expectation 0 (since the y 's are centered), and operator norm bounded by $\max_i \|y_i\| = \rho_\infty$. We are thus in a position to apply [33, Thm 1.6], which gives that, for all $t \geq 0$,

$$\mathbb{P}(\|\bar{z}\| \geq t/\ell) \leq (d+1) \exp\left[-t^2/(2\sigma^2 + \frac{1}{3}\rho_\infty t)\right], \quad (101)$$

where

$$\sigma^2 = (\ell/n)(\|Y^\top Y\| \vee \sum_i \|y_i\|^2) = (\ell/n)\sum_i \|y_i\|^2 \leq \ell\rho_\infty^2. \quad (102)$$

In particular,

$$\mathbb{P}(\|\bar{z}\| \geq \frac{1}{4}\omega^2) \leq (d+1) \exp\left[-\frac{1}{4}\omega^2\ell^2/(2\rho_\infty\ell + \frac{1}{3}\rho_\infty\frac{1}{2}\omega\ell)\right] \quad (103)$$

$$\leq (d+1) \exp\left[-\frac{1}{9}\ell\omega^2/\rho_\infty^2\right], \quad (104)$$

using in the last line the fact that $\omega \leq \rho_\infty$.

Combining these inequalities using the union bound, we conclude that

$$\mathbb{P}(\omega_Z \leq \frac{1}{2}\omega) \leq d \exp\left[-\frac{1}{8}\ell\omega^2/\rho_\infty^2\right] + (d+1) \exp\left[-\frac{1}{9}\ell\omega^2/\rho_\infty^2\right], \quad (105)$$

from which the stated result follows.

Acknowledgements

We are grateful to Vin de Silva, Luis Rademacher, and Ilse Ipsen for helpful discussions and pointers to the literature. Part of this work was performed while the first and second authors were visiting the Simons Institute⁴ on the campus of the University of California, Berkeley. The first author was partially supported by the National Science Foundation (DMS 0915160, 1513465) and the French National Research Agency (ANR 09-BLAN-0051-01). The second author was partially supported by a Google Faculty Research Award.

⁴ The Simons Institute for the Theory of Computing (<https://simons.berkeley.edu>)

References

- [1] E. Arias-Castro and T. L. Gouic. Unconstrained and curvature-constrained shortest-path distances and their approximation. *arXiv preprint arXiv:1706.09441*, 2017.
- [2] E. Arias-Castro and B. Pelletier. On the convergence of maximum variance unfolding. *The Journal of Machine Learning Research*, 14(1):1747–1770, 2013.
- [3] M. Belkin and P. Niyogi. Towards a theoretical foundation for Laplacian-based manifold methods. *Journal of Computer and System Sciences*, 74(8):1289–1308, 2008.
- [4] M. Bernstein, V. De Silva, J. Langford, and J. Tenenbaum. Graph approximations to geodesics on embedded manifolds. Technical report, Technical report, Department of Psychology, Stanford University, 2000.
- [5] P. Biswas, T.-C. Liang, K.-C. Toh, Y. Ye, and T.-C. Wang. Semidefinite programming approaches for sensor network localization with noisy distance measurements. *Transactions on Automation Science and Engineering*, 3(4):360–371, 2006.
- [6] R. Coifman and S. Lafon. Diffusion maps. *Applied and Computational Harmonic Analysis*, 21(1):5–30, 2006.
- [7] V. de Silva and J. Tenenbaum. Global versus local methods in nonlinear dimensionality reduction. *Advances in Neural Information Processing Systems (NIPS)*, 15:705–712, 2003.
- [8] V. de Silva and J. B. Tenenbaum. Sparse multidimensional scaling using landmark points. Technical report, Technical report, Stanford University, 2004.
- [9] D. L. Donoho and C. Grimes. Hessian eigenmaps: Locally linear embedding techniques for high-dimensional data. *Proceedings of the National Academy of Sciences*, 100(10):5591–5596, 2003.
- [10] C. Faloutsos and K.-I. Lin. Fastmap: A fast algorithm for indexing, data-mining and visualization of traditional and multimedia datasets. In *ACM SIGMOD International Conference on Management of Data*, volume 24, pages 163–174, 1995.
- [11] H. Federer. Curvature measures. *Transactions of the American Mathematical Society*, 93:418–491, 1959.
- [12] C. R. Genovese, M. Perone-Pacifico, I. Verdinelli, and L. Wasserman. Manifold estimation and singular deconvolution under hausdorff loss. *The Annals of Statistics*, 40(2):941–963, 2012.
- [13] E. Giné and V. Koltchinskii. Empirical graph Laplacian approximation of laplace–beltrami operators: Large sample results. In *High dimensional probability*, pages 238–259. Institute of Mathematical Statistics, 2006.
- [14] Y. Goldberg, A. Zakai, D. Kushnir, and Y. Ritov. Manifold learning: The price of normalization. *Journal of Machine Learning Research*, 9(Aug):1909–1939, 2008.
- [15] M. Hein, J.-Y. Audibert, and U. Von Luxburg. From graphs to manifolds: Weak and strong pointwise consistency of graph Laplacians. In *Conference on Computational Learning Theory (COLT)*, pages 470–485. Springer, 2005.
- [16] J. T. Holodnak and I. C. Ipsen. Randomized approximation of the gram matrix: Exact computation and probabilistic bounds. *SIAM Journal on Matrix Analysis and Applications*, 36(1):110–137, 2015.
- [17] I. C. Ipsen and T. Wentworth. The effect of coherence on sampling from matrices with orthonormal columns, and preconditioned least squares problems. *SIAM Journal on Matrix Analysis and Applications*, 35(4):1490–1520, 2014.
- [18] A. Javanmard and A. Montanari. Localization from incomplete noisy distance measurements. *Foundations of Computational Mathematics*, 13(3):297–345, 2013.
- [19] A. K. Kim and H. H. Zhou. Tight minimax rates for manifold estimation under hausdorff loss. *Electronic Journal of Statistics*, 9(1):1562–1582, 2015.
- [20] J. B. Kruskal and J. B. Seery. Designing network diagrams. In *General Conference on Social Graphics*, pages 22–50, 1980.
- [21] D. Niculescu and B. Nath. DV based positioning in ad hoc networks. *Telecommunication Systems*, 22(1-4):267–280, 2003.
- [22] A. Paprotny and J. Gacke. On a connection between maximum variance unfolding, shortest path problems and isomap. In *Conference on Artificial Intelligence and Statistics (AISTATS)*, pages 859–867, 2012.
- [23] J. Platt. Fastmap, MetricMap, and Landmark MDS are all Nystrom algorithms. In *Conference on Artificial Intelligence and Statistics (AISTATS)*, 2005.

- [24] G. A. Seber. *Multivariate observations*. John Wiley & Sons, 2004.
- [25] Y. Shang, W. Ruml, Y. Zhang, and M. P. Fromherz. Localization from mere connectivity. In *Symposium on Mobile Ad Hoc Networking & Computing*, pages 201–212, 2003.
- [26] R. Sibson. Studies in the robustness of multidimensional scaling: Perturbational analysis of classical scaling. *Journal of the Royal Statistical Society. Series B (Methodological)*, pages 217–229, 1979.
- [27] A. Singer. From graph to manifold Laplacian: The convergence rate. *Applied and Computational Harmonic Analysis*, 21(1):128–134, 2006.
- [28] A. Smith, X. Huo, and H. Zha. Convergence and rate of convergence of a manifold-based dimension reduction algorithm. In *Advances in Neural Information Processing Systems (NIPS)*, pages 1529–1536, 2008.
- [29] A. M.-C. So and Y. Ye. Theory of semidefinite programming for sensor network localization. *Mathematical Programming*, 109(2-3):367–384, 2007.
- [30] G. W. Stewart and J. G. Sun. *Matrix perturbation theory*. Computer Science and Scientific Computing. Academic Press Inc., Boston, MA, 1990. ISBN 0-12-670230-6.
- [31] J. B. Tenenbaum, V. de Silva, and J. C. Langford. A global geometric framework for nonlinear dimensionality reduction. *Science*, 290(5500):2319–2323, 2000.
- [32] W. S. Torgerson. *Theory and methods of scaling*. Wiley, 1958.
- [33] J. A. Tropp. User-friendly tail bounds for sums of random matrices. *Foundations of Computational Mathematics*, 12(4):389–434, 2012.
- [34] U. von Luxburg, M. Belkin, and O. Bousquet. Consistency of spectral clustering. *The Annals of Statistics*, 36(2):555–586, 2008.
- [35] J. T.-L. Wang, X. Wang, K.-I. Lin, D. Shasha, B. A. Shapiro, and K. Zhang. Evaluating a class of distance-mapping algorithms for data mining and clustering. In *Conference on Knowledge Discovery and Data Mining (SIGKDD)*, pages 307–311, 1999.
- [36] G. Watson. The solution of orthogonal procrustes problems for a family of orthogonally invariant norms. *Advances in Computational Mathematics*, 2(4):393–405, 1994.
- [37] K. Q. Weinberger and L. K. Saul. An introduction to nonlinear dimensionality reduction by maximum variance unfolding. In *Conference on Artificial Intelligence*, volume 2, pages 1683–1686. AAAI, 2006.
- [38] K. Q. Weinberger and L. K. Saul. Unsupervised learning of image manifolds by semidefinite programming. *International Journal of Computer Vision*, 70(1):77–90, 2006.
- [39] K. Q. Weinberger, F. Sha, Q. Zhu, and L. K. Saul. Graph Laplacian regularization for large-scale semidefinite programming. In *Advances in Neural Information Processing Systems (NIPS)*, pages 1489–1496, 2006.
- [40] Q. Ye and W. Zhi. Discrete hessian eigenmaps method for dimensionality reduction. *Journal of Computational and Applied Mathematics*, 278:197–212, 2015.
- [41] F. W. Young. *Multidimensional scaling: History, theory, and applications*. Psychology Press, 2013.
- [42] H. Zha and Z. Zhang. Continuum isomap for manifold learnings. *Computational Statistics & Data Analysis*, 52(1):184–200, 2007.